

Analog time machine in a photonic systemD. D. Solnyshkov^{1,2} and G. Malpuech¹¹*Institut Pascal, PHOTON-N2, Université Clermont Auvergne, CNRS, SIGMA Clermont, F-63000 Clermont-Ferrand, France*²*Institut Universitaire de France (IUF), F-75231 Paris, France*

(Received 20 November 2020; revised 25 January 2021; accepted 26 January 2021; published 10 February 2021)

Analog physics has successfully tackled the problems of gauge theories, event horizons, Big Bang and Universe expansion, and many others. Here, we suggest a photonic model system for a “time machine” based on the paraxial beam approximation. We demonstrate how the closed timelike curves and the well-known grandfather paradox can be studied experimentally in this system. We show how Novikov’s self-consistency principle is realized in quantum mechanics owing to Heisenberg’s uncertainty principle.

DOI: [10.1103/PhysRevB.103.054303](https://doi.org/10.1103/PhysRevB.103.054303)**I. INTRODUCTION**

Analog physics is based on the mathematical similarities between different physical systems. These analogies often help to solve long-standing problems in some fields, by bringing the solutions known in the other fields. Among the most well-known examples of the success of such analogies are Maxwell’s equations (derived by analogy with the fluid dynamics in the presence of vortices) [1], Anderson’s suggestion [2] for the mass generation of gauge bosons by symmetry breaking via what is now known as the Higgs mechanism [3] (based on the analogy with superconductors), and Semenoff’s proposal for the realization of Dirac’s Hamiltonian in graphene [4] with the associated effect of Klein tunneling [5], which stimulated the works on graphene [6]. One of the particularly developed fields of analog physics is analog gravity [7,8]. Thirty years after the initial proposal of Unruh [9] for the observation of an analog of Hawking emission [10] expected to arise at event horizons, such emission has indeed been observed experimentally in classical [11,12] and quantum fluids [13,14]. The studies of analog spacetimes are not limited to Hawking emission: They include also superradiance [15] and the Penrose effect [16] for Kerr black holes, the Big Bang and the expansion [17–19], analog wormholes [20–22], and even false vacuum decay [23,24].

A very interesting conclusion of the general relativity is the possibility of the existence of closed timelike curves (CTCs), commonly called “time machines” [25]. Indeed, the relativity of simultaneity implies that there is no common “now” for the whole Universe, and therefore that different moments of time coexist, and can possibly be traveled to. Soon after the discovery of the wormhole-type solutions of Einstein’s equations for the spacetime metric [26,27], it was understood that traversable wormholes [28,29] allowed faster-than-light travel, which, in turn, makes time travel possible [25]. Moreover, it seems that any faster-than-light travel, which is a goal of current NASA projects [30], appears as backward time motion for some observers. CTCs are the spacetime trajectories of objects traveling through a time machine: Their closed character implies the possibility for the object to affect its

own past. The most well-known theoretical result concerning CTCs is Novikov’s self-consistency principle stating that the only events which can occur along such closed curves are those which are globally self-consistent [31]. These works have inspired a strong research activity on both classical [32] and quantum [33] problems in the presence of time machines, including the problem of free will [34]. In quantum mechanics with CTCs, many counterintuitive results were obtained, such as the solution of *NP*-complete problems in polynomial time [35]. Recently, the interaction of a qubit with another one trapped in a CTC has been simulated experimentally, marking another milestone for analog physics [36]. The long-standing question of causality, free will, and the possibility of changing one’s own past has moved from the realm of philosophical problems into the dominion of experimental physics.

Photonics offers extended possibilities for analog physics, including analog spacetimes [37]. The whole field of topological photonics [38,39] was born from the possibility to simulate wave functions in periodic crystal lattices using electromagnetic waves in artificially constructed periodic media. The advantage of photonics is the opportunity to observe wave functions experimentally (including the phase) and to perform wave-function engineering with artificial potentials, e.g., periodic lattices. As an example, the possibilities to simulate electromagnetic wormholes with metamaterials were recently suggested [40,41]. In particular, the well-known paraxial approximation for light has been used for analog physics studies in atomic vapor cells [42,43], nonlinear crystals [44], and in coupled waveguides [45].

In this paper, we propose to study the self-consistency of time travel by using the equivalence between the time coordinate in the Schrödinger equation and one of the space coordinates (the *z* coordinate, corresponding to the beam propagation direction) in a paraxial configuration. We show with numerical simulations that the system indeed converges to a stationary self-consistent solution, confirming Novikov’s principle, which is realized owing to the inherent quantum uncertainty. We demonstrate that in the stationary case, the time-looped signal can be either self-amplified or self-suppressed. We show that this suppression can never be

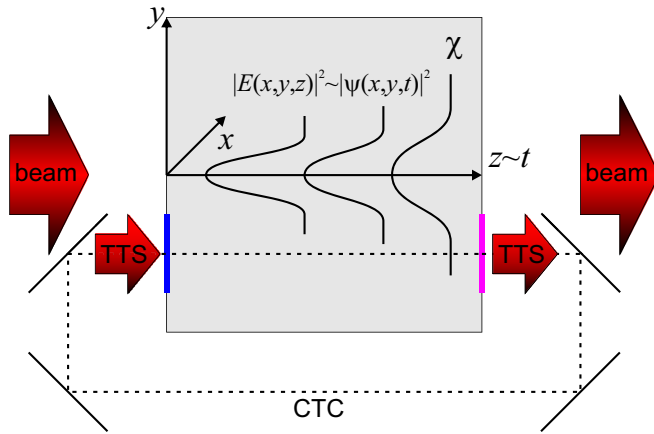


FIG. 1. Scheme of the experiment. The dielectric medium characterized by susceptibility χ is shown as a gray rectangle. The input beam arrives from the left. The z -dependent envelope of the electric field $E(x, y, z)$ behaves as a time-dependent wave function $\psi(x, y, t)$, its diffusion sketched with black lines. The output region marked with a magenta line is transferred to the input region marked with a blue line using four mirrors (Mach-Zehnder interferometer setup). The time-traveler signal (TTS) goes around the closed timelike curve (CTC) marked with a dashed line.

complete. Traveling to the past and killing the younger version of yourself is therefore impossible.

II. THE MODEL

The paraxial approximation consists in considering the envelope of an electric field and neglecting $\partial^2 \mathbf{E}_\perp / \partial z^2$ with respect to $k_0 \partial \mathbf{E}_\perp / \partial z$ in the Laplacian term of the Helmholtz equation for the electromagnetic field. The resulting equation for the envelope (neglecting the spin-orbit coupling effects) reads

$$i \frac{\partial E}{\partial z} = -\frac{1}{2k_0} \left(\frac{\partial^2}{\partial x^2} + \frac{\partial^2}{\partial y^2} \right) E - \frac{k_0 \chi}{2} E, \quad (1)$$

where χ is the dielectric susceptibility of the medium and k_0 is the propagation wave vector along z . This equation is equivalent to the time-dependent two-dimensional (2D) Schrödinger equation

$$i\hbar \frac{\partial \psi}{\partial t} = -\frac{\hbar^2}{2m} \Delta \psi + U \psi, \quad (2)$$

with the mass m determined by k_0 and the potential U determined by the susceptibility profile χ . Nonlinear terms can be present in both equations. Their role will be considered in the following sections. It is because of the paraxial approximation that the derivatives over z and x, y appear differently in this equation, which corresponds to the difference between the spatial coordinates and the time (in particular, in the nonrelativistic limit, in which the Schrödinger equation is written).

The z coordinate of Eq. (1) maps to the time variable in the Schrödinger equation (2). We propose to use this mapping to create a model of a CTC or a time machine by coupling the output of the medium to its input, as shown in Fig. 1. This analog system is not supposed to reproduce the wormhole itself, which is a relativistic object, but rather its effect on

the asymptotically flat regions of spacetime. The initial beam from the source enters the medium described by Eqs. (1) and (2) from the left. The evolution of the electric field envelope (or wave function) with z (analog time) is sketched by a black solid line. A set of four mirrors (forming a Mach-Zehnder interferometer) loops a part of the beam from the output on the right back to the entrance on the left, forming the CTC (dashed line). Only the internal part of the CTC is simulated in the analog system, whereas the external part (the wormhole) is supposed to transmit the signal with minimal changes (as expected for a time machine). Our configuration quite faithfully reproduces such an imaginary device, because the wave packet is actually described by the same equation (corresponding to the nonrelativistic limit of a flat Minkowski spacetime) along all four parts of the optical path. Indeed, an object moving through a wormhole is supposed to be still moving forward in time in its local frame, while going backward with respect to an external observer. We note that the requirement of minimal changes during “time travel” might imply using a different refractive index for the main part of the system, in order to increase the relative weight of the useful “forward” optical path with respect to the “backward” outside path.

III. LINEAR MEDIUM

We begin by considering the problem of a possible stationary solution for the electric field envelope $E(x, y, z)$ equivalent to the existence of a stable history of the Universe $\psi(x, y, t)$ mathematically. Let us consider that the signal from a single point x_0, y_0 at the moment T given by $\psi(x_0, y_0, T)$ is sent backward into the past to the same point at the moment $t = 0$ and adds to the wave function already existing at that moment as

$$\psi(x_0, y_0, 0) \leftarrow \psi(x_0, y_0, 0) + \alpha \psi(x_0, y_0, T), \quad (3)$$

where α is a complex coefficient describing the efficiency of the time machine. In a realistic optical system without gain, $|\alpha| \leq 1$, but in principle it can also exceed unity. The most efficient way to find a stationary solution for E is to use iterations: Solve the time-dependent equation for ψ from $t = 0$ to $t = T$, and then use $\psi(x_0, y_0, T)$ as the input for the next iteration. We can therefore write

$$\psi_{n+1}(x_0, y_0, 0) = \psi_n(x_0, y_0, 0) + \alpha \psi_n(x_0, y_0, T). \quad (4)$$

From a mathematical point of view, the values of the signal sent backward (describing the state of the time traveler) represent a sequence. This sequence is either convergent or not. If it converges to a certain limit $\psi_n(x_0, y_0, T) \rightarrow c$, four interesting situations are possible at first glance: (1) $c = 0$, complete suppression of the time-traveler signal (TTS); (2) $|c| < |\psi_0(x_0, y_0, T)|$, partial suppression of the TTS; (3) $|c| > |\psi_0(x_0, y_0, T)|$, limited amplification of the TTS; and (4) $c = \infty$, unlimited amplification of the TTS.

Let us first focus on the first possibility, which corresponds precisely to the time-traveler (or grandfather) paradox: Is it possible to kill one’s own younger self? The answer that we can prove mathematically is no. Indeed, let us suppose that $c = \lim \psi_n(x_0, y_0, T) = 0$. By definition, it means that there exists an N such that for $n > N$, $|\psi_n(x_0, y_0, T)| < \epsilon$ (with

arbitrary small ϵ). Then, for the next iteration $n + 1$ at $t = 0$ we have an initial value which is arbitrarily close to the *zeroth* (that is, initial) iteration,

$$|\psi_{n+1}(x_0, y_0, 0) - \psi_0(x_0, y_0, 0)| < |\alpha|\epsilon, \quad (5)$$

because this initial value is given by

$$\psi_{n+1}(x_0, y_0, 0) = \psi_0(x_0, y_0, 0) + \alpha\psi_n(x_0, y_0, T). \quad (6)$$

For any finite $|\alpha|$, the product $|\alpha|\epsilon$ can be made arbitrarily small. Next, we apply the Lyapunov analysis of stability [46]. If the original system (without the CTC) is stable (not chaotic) and all its Lyapunov exponents are negative, the arbitrarily small separation of initial conditions (at $t = 0$) implies an even smaller separation of the final values (at the moment T):

$$|\psi_{n+1}(x_0, y_0, T) - \psi_0(x_0, y_0, T)| < |\psi_{n+1}(x_0, y_0, 0) - \psi_0(x_0, y_0, 0)| < |\alpha|\epsilon. \quad (7)$$

We find therefore that ψ_{n+1} is arbitrarily close to zero and at the same time to the zeroth iteration value $\psi_0(x_0, y_0, T)$, which is impossible, unless $\psi_0(x_0, y_0, T) = 0$ (there was no time traveler from the start, which is a trivial situation). We must conclude that the signal sent to the past cannot suppress itself completely.

The three other configurations are possible mathematically. We note, however, that the infinite self-amplification is impossible in a physical implementation of an analog time machine that we suggest because of the inevitable gain saturation mechanisms. We conclude that, in practice, the TTS is either partially suppressed or amplified.

It is also possible that the sequence ψ_n does not converge at all: The stationary configuration of the electromagnetic field does not settle down in the system. This can occur if the original system has a positive Lyapunov exponent (exhibits a chaotic behavior), because in this case even a weak signal into the past strongly modifies the future, including itself. The possibility of the creation of such a configuration in an analog system in the quantum case that requires dynamical quantum chaos [47] remains an open question that we leave for future works.

We have to stress that we restrict our consideration to the case of a negligible beam evolution outside the dielectric (ensured by the difference of the refractive indices). Indeed, if the optical path outside the dielectric medium is significant, the changes in the spatial profile of the reinjected beam (with respect to the output profile) can become non-negligible. In this case, our initial assumption is not valid, and the whole reasoning should no longer be applied. The analogy with a “time machine” still remains valid, but the causal links are more complicated.

Figure 2 shows the results of numerical simulations based on the linear time-dependent Schrödinger equation with a Gaussian profile of the beam (width w) and a Gaussian spatial profile of the CTC (qualitatively describing the mirrors shown in Fig. 1), coupling the final value of the wave function $\psi(y, T)$ into its initial value $\psi(y, 0)$. The problem is reduced to 1D (the system is considered to be homogeneous along x) in order to focus on its essential features. The simulations confirm the possibility of the achievement of a stationary solution for the electromagnetic field, an equivalent of a self-consistent

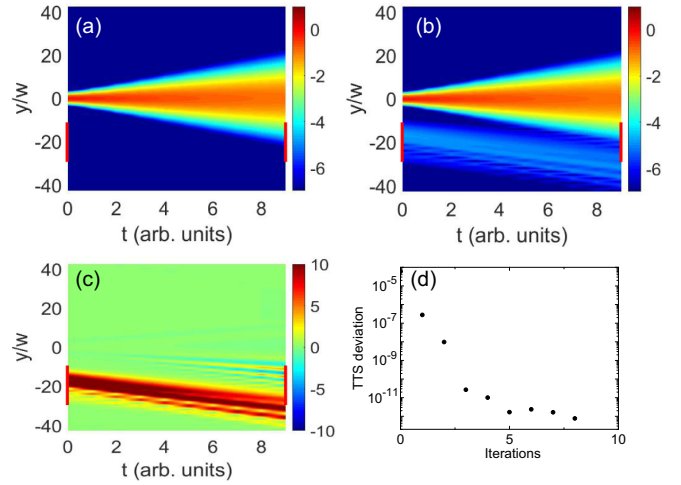


FIG. 2. Numerical simulations. (a) Initial distribution of $|\psi(y, t)|^2$ (without CTC), log scale. (b) Final stationary distribution of $|\psi(y, t)|^2$ (with CTC), log scale. (c) Difference between the initial and the stationary distributions, linear scale. (d) Convergence of the TTS integrated density with iteration number. Red lines mark the CTC windows.

history in the presence of a CTC. Figure 2(a) shows the initial distribution of the probability density $|\psi(y, t)|^2$ (no CTC), while Fig. 2(b) shows the stationary distribution. The TTS is clearly visible in the bottom part of the figure. It presents a nonzero wave vector oriented downward, because only such components (present in the original beam) can penetrate into the CTC window located at around $y/w = -20$. Figure 2(c) shows the difference of the probability density between the initial and the stationary configurations. The TTS appears as red (local probability increase), but blue regions are also visible: The TTS locally exhibits a negative interference with the initial beam. Finally, Fig. 2(d) demonstrates the convergence of the system: The deviation from the final (stationary) solution drops down to the machine precision in just about five iterations. The sequence $\psi_n(x_0, y_0, T)$ converges to a value about 11% larger than the initial value $\psi_0(x_0, y_0, T)$. This numerical simulation confirms that a stationary solution can be found in this case and that the system can exhibit a self-consistent history, at least in the linear case.

The fast convergence is ensured not only by the fact that this simplest quantum system is not chaotic, but even stronger by its diffractive nature. The spreading of the wave packets guarantees that $|\psi_n(x_0, y_0, T)|^2 < |\psi_n(x_0, y_0, 0)|^2$, which means that the TTS is weakened with each iteration, and thus the sequence rapidly converges. The nonrelativistic quantum mechanics with a CTC appears to respect the self-consistency principle.

A less trivial example is shown in Fig. 3: The wave packet has a nonzero initial wave vector along y [Fig. 3(a), $k_y < 0$], directed towards the time machine (red line). It enters the time machine and reappears at $t = 0$, still directed downwards. Then the wave packet is reflected at a potential barrier at the boundary of the system and gets a new wave vector $k_y > 0$ directed upward. It then reenters the CTC and reappears at $t = 0$ once again, this time continuing to propagate upward. *Three* copies of the same wave packet are present in the system at

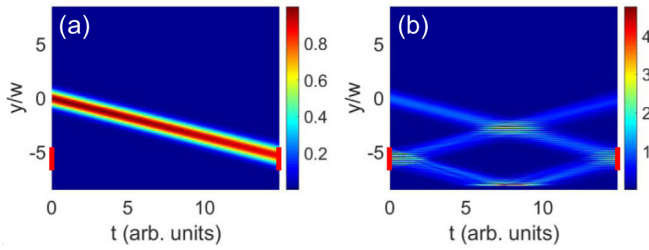


FIG. 3. Numerical simulations showing a more complicated configuration with an initially propagating wave packet. (a) Initial distribution of $|\psi(y, t)|^2$ (without CTC), linear scale. (b) Final stationary distribution of $|\psi(y, t)|^2$ (with CTC), linear scale. Red lines mark the CTC windows.

any moment of time. This configuration is close to that of the classical billiard ball problems [31], with a time-traveling billiard ball hitting a previous version of itself. One could expect that the wave packets might interfere destructively at some point, either at $t = 0$ or at $t = T$, and thus suppress the TTS, but this does not happen, because of the nonzero wave vector: Actually, an interference pattern between positive and negative k_y is observed at $t = 0$ and at $t = T$, and an extra phase simply shifts this interference upward or downward, but it does not lead to the complete suppression of the TTS. The convergence in this case is as fast as in the configuration of Fig. 2.

The most self-affecting configuration corresponds to a wide beam with $k_y = 0$, exhibiting almost no diffraction and entering straight into the CTC, as shown in Fig. 4. This beam reappears at $t = 0$ with the same wave vector $k_y = 0$ and thus reenters the CTC again and again. Two limiting cases are possible: The phase of the CTC coupling coefficient $\phi = \arg \alpha$ can be either zero [constructive interference, Figs. 4(a) and 4(c)] or π [destructive interference, Figs. 4(b) and 4(d)]. In the first case, we could expect that the wave packet might exhibit unlimited amplification and thus no

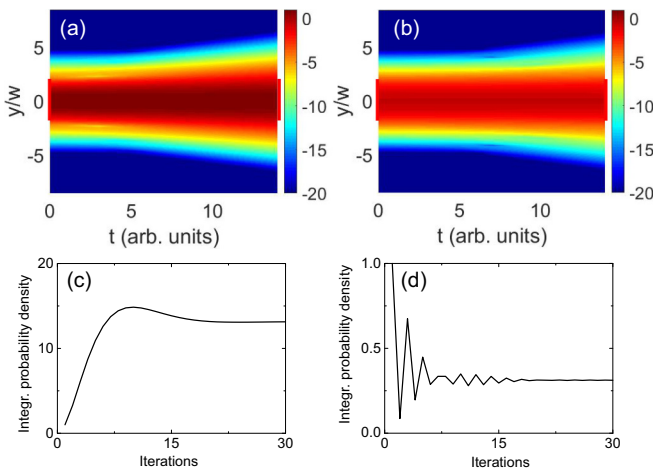


FIG. 4. Numerical simulations of the strongest self-affecting configuration. (a), (b) Final stationary distribution of $|\psi(y, t)|^2$ (with CTC), log scale. Coupling phase: (a) $\phi = 0$, (b) $\phi = \pi$. (c), (d) Corresponding total probability density exhibiting convergence.

stationary solution could be reached. This does not happen, as can be seen from Fig. 4(c), showing the integrated probability density, whose value saturates around 12 (twelve copies of the wave packet simultaneously present in the system). Such cases are rarely treated in science fiction literature (but see, e.g., Ref. [48]). Diffraction prevents a further increase of the self-amplification. Similarly, diffraction prevents the complete suppression of the beam in Fig. 4(b) ($\phi = \pi$). The main part of the beam is strongly suppressed, and the integrated probability initially drops down to ≈ 0.1 , meaning that the time traveler managed to kill its own former self by about 90%. But complete suppression does not occur, in agreement with our analytical predictions. The system converges in about 30 iterations to a value of about 30% of the initial wave packet, exhibiting a strongly broadened spatial distribution. We can conclude that Novikov's self-consistency principle is ensured in quantum mechanics by Heisenberg's uncertainty principle.

IV. NONLINEAR MEDIUM

The paraxial propagation of a beam in a nonlinear medium is described by the nonlinear Schrödinger equation,

$$i\hbar \frac{\partial \psi}{\partial t} = -\frac{\hbar^2}{2m} \Delta \psi + g|\psi|^2 \psi + U \psi. \quad (8)$$

Depending on the sign of the nonlinearity, the interactions (characterized by the constant g) can be either attractive ($g < 0$, in which case the system is unstable) or repulsive ($g > 0$). The evolution of long-wavelength weak excitations (characterized by a speed of sound $c_s = \sqrt{gn/m}$) in such a system can be described using a relativistic wave equation [49],

$$\partial_\nu (\sqrt{-g} g^{\mu\nu} \partial_\nu \varphi) = 0, \quad (9)$$

written with an effective metric tensor $g_{\mu\nu}$ totally determined [9] by the background stationary velocity $\mathbf{v} = (\hbar/m)\nabla \arg \psi$ and the local speed of sound c_s :

$$g_{\mu\nu} = \frac{mn}{c} \begin{pmatrix} -(c^2 - \mathbf{v}^2) & \vdots & -\mathbf{v} \\ \dots\dots\dots & \cdot & \dots\dots\dots \\ -\mathbf{v} & \vdots & \delta_{ij} \end{pmatrix}. \quad (10)$$

It is already widely used for the analog studies of general relativity, including time-related effects. This regime allows us to map the electromagnetic wave in a nonlinear medium not to the nonrelativistic quantum mechanics, as in the previous section, but to a relativistic wave equation for light. Moreover, this nonlinear system also admits another type of nontrivial solution: solitons, localized density perturbations characterized by a phase jump and behaving as relativistic massive particles [50]. These have also already been used for analog studies [51,52].

We note that in this case the physical signal to be sent along the CTC in the analog system should be taken as a deviation from the mean value of the electric field, and not the total electric field as in (3):

$$\psi(x_0, y_0, 0) \leftarrow \psi(x_0, y_0, 0) + \alpha[\psi(x_0, y_0, T) - \bar{\psi}(x, y, T)]. \quad (11)$$

This is best achieved in a pump-probe configuration, where the pump can be suppressed by interference.

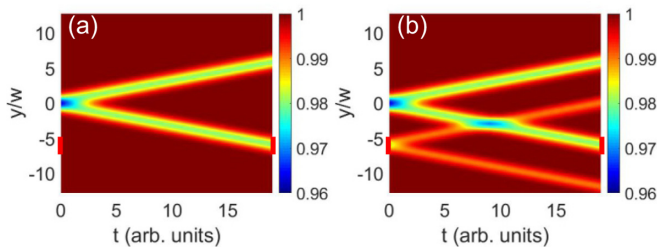


FIG. 5. Numerical simulations for a nonlinear system. (a) Initial distribution of $|\psi(y, t)|^2$ (without CTC), linear scale. (b) Final stationary distribution of $|\psi(y, t)|^2$ (with CTC), linear scale. Red lines mark the CTC windows.

This analog system is much closer to the problems of general relativity and exhibits a much richer behavior than the linear system. In particular, it is possible to simulate the configuration of the billiard ball striking the former version of itself [32] using shallow solitons. They have the advantage of being relatively weakly interacting and propagating almost at the speed of sound. Their presence also does not significantly perturb the phase of the condensate.

Figure 5 shows the results of numerical simulations of shallow soliton propagation in a nonlinear system. The initially created density minimum separates into two gray solitons propagating almost at the speed of sound in the medium c_s . One of them enters a CTC and reappears at $t = 0$, generating two more shallow solitons, the trajectory of one which crosses one of the initial solitons [Fig. 5(b)]. At high speeds, the interaction between the solitons is relatively weak, and even though it leads to a slight deviation of the first soliton, it does not prevent it from entering the CTC. Thus, the time traveler does not destroy itself completely once again, and the system exhibits a self-consistent history.

The characteristic speed of the propagation of the changes in the history in this model system is fundamentally different from the analog of the speed of light. Indeed, the role of the speed of light is played by c_s , whereas the changes propagate from the past to the future along the equivalent of the time axis z with the speed of light in the medium c/n . It means that a change in the past does not affect the time traveler immediately, and for some moment (of the laboratory time) the traveler “remembers” the previous version of the history.

V. DISCUSSION

If the past, the present, and the future exist simultaneously, it means the future “already” exists, and our free will arises

only from the impossibility to predict the future (which is already existing anyway). In this case, the only possibility of a real change in the Universe is given by time machines. Time travel changes history and thus changes the past and the future. On the other hand, the final (stationary) version of a history in the presence of a time machine is not so different from what we actually experience. We have seen that a signal from the future can change history in a quite significant way, and the only certain point is that this signal cannot disappear completely as a result of these changes. But history does not keep track of its initial version, and only the final one can be observed.

Ultimately, any time machine can be represented as a system with feedback in a stationary equilibrium configuration. The behavior of systems with a feedback has been studied by control theory in many works. Our own brain is a complicated feedback system, and in this sense, works as a time machine: We conceive a certain future which is ultimately not realized, because we get some information from this potential future and adapt our behavior correspondingly, in order to optimize the outcomes. But the realized version of history contains our “mind simulations” and the feedback signal that we have received from them as a part of our personal history.

VI. CONCLUSIONS

To conclude, we have shown that it is possible to simulate “time machines” or systems with closed timelike curves, using electromagnetic beams in the paraxial configuration, mapped to a time-dependent Schrödinger equation. We have shown that it is possible to check Novikov’s self-consistency principle experimentally in such systems. Our analysis demonstrates how the time-traveler (or the grandfather) paradox is resolved in quantum mechanics. We have shown that the self-consistency is ultimately achieved owing to Heisenberg’s uncertainty principle. However, it might be violated in systems with dynamical quantum chaos.

ACKNOWLEDGMENT

We acknowledge the support of the projects EU “QUANTOPOL” (846353), “Quantum Fluids of Light” (ANR-16-CE30-0021), of the ANR Labex GaNEXT (ANR-11-LABX-0014), and of the ANR program “Investissements d’Avenir” through the IDEX-ISITE initiative 16-IDEX-0001 (CAP 20-25).

- [1] J. C. Maxwell, On physical lines of force, *Philos. Mag.* **90**, 11 (1861).
- [2] P. W. Anderson, Plasmons, gauge invariance, and mass, *Phys. Rev.* **130**, 439 (1963).
- [3] P. W. Higgs, Broken Symmetries and the Masses of Gauge Bosons, *Phys. Rev. Lett.* **13**, 508 (1964).
- [4] G. W. Semenoff, Condensed-Matter Simulation of a Three-Dimensional Anomaly, *Phys. Rev. Lett.* **53**, 2449 (1984).

- [5] O. Klein, Die reflexion von elektronen an einem potentialsprung nach der relativistischen dynamik von Dirac, *Z. Phys.* **53**, 157 (1929).
- [6] M. Katsnelson, K. Novoselov, and A. Geim, Chiral tunneling and the Klein paradox in graphene, *Nat. Phys.* **2**, 620 (2006).
- [7] C. Barceló, S. Liberati, and M. Visser, Analogue gravity, *Living Rev. Relativ.* **8**, 12 (2005).
- [8] C. Barcelo, Analogue black-hole horizons, *Nat. Phys.* **15**, 210 (2019).

- [9] W. G. Unruh, Experimental Black-Hole Evaporation?, *Phys. Rev. Lett.* **46**, 1351 (1981).
- [10] S. W. Hawking, Black hole explosions? *Nature (London)* **248**, 30 (1974).
- [11] S. Weinfurter, E. W. Tedford, M. C. J. Penrice, W. G. Unruh, and G. A. Lawrence, Measurement of Stimulated Hawking Emission in an Analogue System, *Phys. Rev. Lett.* **106**, 021302 (2011).
- [12] L.-P. Euvé, F. Michel, R. Parentani, T. G. Philbin, and G. Rousseaux, Observation of Noise Correlated by the Hawking Effect in a Water Tank, *Phys. Rev. Lett.* **117**, 121301 (2016).
- [13] J. Steinhauer, Observation of self-amplifying Hawking radiation in an analogue black-hole laser, *Nat. Phys.* **10**, 864 (2014).
- [14] J. R. M. de Nova, K. Golubkov, V. I. Kolobov, and J. Steinhauer, Observation of thermal Hawking radiation and its temperature in an analogue black hole, *Nature (London)* **569**, 688 (2019).
- [15] T. Torres, S. Patrick, A. Coutant, M. Richartz, E. W. Tedford, and S. Weinfurter, Rotational superradiant scattering in a vortex flow, *Nat. Phys.* **13**, 833 (2017).
- [16] D. D. Solnyshkov, C. Leblanc, S. V. Koniakhin, O. Bleu, and G. Malpuech, Quantum analogue of a Kerr black hole and the Penrose effect in a Bose-Einstein condensate, *Phys. Rev. B* **99**, 214511 (2019).
- [17] U. R. Fischer and R. Schützhold, Quantum simulation of cosmic inflation in two-component Bose-Einstein condensates, *Phys. Rev. A* **70**, 063615 (2004).
- [18] S. Eckel, A. Kumar, T. Jacobson, I. B. Spielman, and G. K. Campbell, A Rapidly Expanding Bose-Einstein Condensate: An Expanding Universe in the Lab, *Phys. Rev. X* **8**, 021021 (2018).
- [19] G. Rousseaux and S. C. Mancas, Visco-elastic cosmology for a sparkling universe? *Gen. Relativ. Gravit.* **52**, 1 (2020).
- [20] D. D. Solnyshkov, H. Flayac, and G. Malpuech, Black holes and wormholes in spinor polariton condensates, *Phys. Rev. B* **84**, 233405 (2011).
- [21] C. Peloquin, L.-P. Euvé, T. Philbin, and G. Rousseaux, Analog wormholes and black hole laser effects in hydrodynamics, *Phys. Rev. D* **93**, 084032 (2016).
- [22] L.-P. Euvé and G. Rousseaux, Classical analogue of an interstellar travel through a hydrodynamic wormhole, *Phys. Rev. D* **96**, 064042 (2017).
- [23] J. Braden, M. C. Johnson, H. V. Peiris, A. Pontzen, and S. Weinfurter, Nonlinear dynamics of the cold atom analog false vacuum, *J. High Energy Phys.* **10** (2019) 174.
- [24] T. P. Billam, R. Gregory, F. Michel, and I. G. Moss, Simulating seeded vacuum decay in a cold atom system, *Phys. Rev. D* **100**, 065016 (2019).
- [25] M. S. Morris, K. S. Thorne, and U. Yurtsever, Wormholes, Time Machines, and the Weak Energy Condition, *Phys. Rev. Lett.* **61**, 1446 (1988).
- [26] A. Einstein and N. Rosen, The particle problem in the general theory of relativity, *Phys. Rev.* **48**, 73 (1935).
- [27] R. W. Fuller and J. A. Wheeler, Causality and multiply connected space-time, *Phys. Rev.* **128**, 919 (1962).
- [28] H. G. Ellis, Ether flow through a drainhole: A particle model in general relativity, *J. Math. Phys.* **14**, 104 (1973).
- [29] K. Bronnikov, Scalar-tensor theory and scalar charge, *Acta Phys. Polon. B* **4**, 251 (1973).
- [30] H. White, Warp Field Physics, Technical Report No. JSC-CN-29229, NASA, Washington, DC, 2013.
- [31] J. Friedman, M. S. Morris, I. D. Novikov, F. Echeverria, G. Klinkhammer, K. S. Thorne, and U. Yurtsever, Cauchy problem in spacetimes with closed timelike curves, *Phys. Rev. D* **42**, 1915 (1990).
- [32] F. Echeverria, G. Klinkhammer, and K. S. Thorne, Billiard balls in wormhole spacetimes with closed timelike curves: Classical theory, *Phys. Rev. D* **44**, 1077 (1991).
- [33] D. Deutsch, Quantum mechanics near closed timelike lines, *Phys. Rev. D* **44**, 3197 (1991).
- [34] G. Tobar and F. Costa, Reversible dynamics with closed timelike curves and freedom of choice, *Classical Quantum Gravity* **37**, 205011 (2020).
- [35] D. Bacon, Quantum computational complexity in the presence of closed timelike curves, *Phys. Rev. A* **70**, 032309 (2004).
- [36] M. Ringbauer, M. A. Broome, C. R. Myers, A. G. White, and T. C. Ralph, Experimental simulation of closed timelike curves, *Nat. Commun.* **5**, 4145 (2014).
- [37] M. Jacquet, T. Boulier, F. Claude, A. Maître, E. Cancellieri, C. Adrados, A. Amo, S. Pigeon, Q. Glorieux, A. Bramati *et al.*, Polariton fluids for analogue gravity physics, *Philos. Trans. R. Soc. A* **378**, 20190225 (2020).
- [38] L. Lu, J. D. Joannopoulos, and M. Soljačić, Topological photonics, *Nat. Photonics* **8**, 821 (2014).
- [39] T. Ozawa, H. M. Price, A. Amo, N. Goldman, M. Hafezi, L. Lu, M. C. Rechtsman, D. Schuster, J. Simon, O. Zilberberg, and I. Carusotto, Topological photonics, *Rev. Mod. Phys.* **91**, 015006 (2019).
- [40] A. Greenleaf, Y. Kurylev, M. Lassas, and G. Uhlmann, Electromagnetic Wormholes and Virtual Magnetic Monopoles from Metamaterials, *Phys. Rev. Lett.* **99**, 183901 (2007).
- [41] J. Prat-Camps, C. Navau, and A. Sanchez, A magnetic wormhole, *Sci. Rep.* **5**, 12488 (2015).
- [42] Z. Zhang, Y. Zhang, J. Sheng, L. Yang, M.-A. Miri, D. N. Christodoulides, B. He, Y. Zhang, and M. Xiao, Observation of Parity-Time Symmetry in Optically Induced Atomic Lattices, *Phys. Rev. Lett.* **117**, 123601 (2016).
- [43] Z. Zhang, F. Li, G. Malpuech, Y. Zhang, O. Bleu, S. Koniakhin, C. Li, Y. Zhang, M. Xiao, and D. D. Solnyshkov, Particlelike Behavior of Topological Defects in Linear Wave Packets in Photonic Graphene, *Phys. Rev. Lett.* **122**, 233905 (2019).
- [44] D. Vocke, C. Maitland, A. Prain, K. E. Wilson, F. Biancalana, E. M. Wright, F. Marino, and D. Faccio, Rotating black hole geometries in a two-dimensional photon superfluid, *Optica* **5**, 1099 (2018).
- [45] M. C. Rechtsman, J. M. Zeuner, Y. Plotnik, Y. Lumer, D. Podolsky, F. Dreisow, S. Nolte, M. Segev, and A. Szameit, Photonic Floquet topological insulators, *Nature (London)* **496**, 196 (2013).
- [46] J. P. Eckmann and D. Ruelle, Ergodic theory of chaos and strange attractors, *Rev. Mod. Phys.* **57**, 617 (1985).
- [47] B. Pokharel, M. Z. Misplon, W. Lynn, P. Duggins, K. Hallman, D. Anderson, A. Kapulkin, and A. K. Pattanayak, Chaos and dynamical complexity in the quantum to classical transition, *Sci. Rep.* **8**, 1 (2018).

- [48] S. Lem, *The Star Diaries* (Penguin Classics, London, 2016).
- [49] L. J. Garay, J. R. Anglin, J. I. Cirac, and P. Zoller, Sonic Analog of Gravitational Black Holes in Bose-Einstein Condensates, *Phys. Rev. Lett.* **85**, 4643 (2000).
- [50] L. Pitaevskii and S. Stringari, *Bose-Einstein Condensation*, International Series of Monographs on Physics Vol. 116 (Oxford Science Publications, Oxford, UK, 2003).
- [51] D. D. Solnyshkov, H. Flayac, and G. Malpuech, Stable magnetic monopoles in spinor polariton condensates, *Phys. Rev. B* **85**, 073105 (2012).
- [52] R. Hivet, H. Flayac, D. D. Solnyshkov, D. Tanese, T. Boulier, D. Andreoli, E. Giacobino, J. Bloch, A. Bramati, G. Malpuech, and A. Amo, Half-solitons in a polariton quantum fluid behave like magnetic monopoles, *Nat. Phys.* **8**, 724 (2012).